



Mechanism of the cobalt-catalyzed carbonylation of ethyl diazoacetate

Neszta Ungvári, Eszter Fördös, Tamás Kégl, Ferenc Ungváry *

Department of Organic Chemistry, University of Pannonia, 8201 Veszprém, Egyetem u. 10, Hungary

ARTICLE INFO

Article history:

Received 27 February 2009

Received in revised form 28 August 2009

Accepted 11 September 2009

Available online 16 September 2009

Dedicated to Professor László Markó on the occasion of his 80th birthday.

Keywords:

Cobalt
Carbene and carbonyl ligands
C–C coupling
Ketene
Density functional calculations

ABSTRACT

Carbonyl cobalt complexes serve as catalysts or catalyst precursors for the facile and selective transformation of primary diazoalkanes into the corresponding ketene. The mechanism of this carbonylation reaction has been elucidated in the case of ethyl diazoacetate as model diazoalkane using octacarbonyl dicobalt as the catalyst precursor. Dinuclear cobalt complexes having ethoxycarbonylcarbene ligand(s) in bridging position(s) have been identified as active intermediary of the catalytic cycles and their relevant chemical properties have been explored. Key step of the carbonylation is the formation of the highly reactive ethoxycarbonylketene by intramolecular coupling of a carbonyl ligand with the ethoxycarbonylcarbene ligand. DFT calculations reveal that the ketene formation takes place via a rapid coupling of the carbene ligand with one terminal CO followed by coordination of an external carbon monoxide and by a facile intramolecular rearrangement and ketene elimination. The ethoxycarbonylketene can be *in situ* trapped by OH, NH, or CH acid compounds or by *N*-substituted imines. In the presence of ethanol diethyl malonate is the only product of the catalytic carbonylation of ethyl diazoacetate. On the bases of the kinetics of the composing steps of the catalytic cycles, localization of the rate-determining step(s) under various reaction conditions has been made.

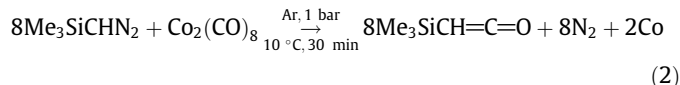
© 2009 Elsevier B.V. All rights reserved.

1. Introduction

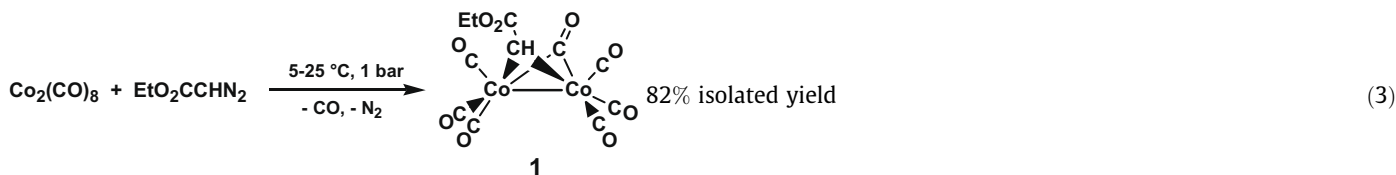
Octacarbonyl dicobalt was found to be an effective dediazotation reagent for (trimethylsilyl)diazomethane [1] or ethyl diazoacetate [2]. In the dediazotation reaction of (trimethylsilyl)diazomethane with $\text{Co}_2(\text{CO})_8$ (trimethylsilyl)ketene is formed selectively either under catalytic (reaction 1) or under stoichiometric (reaction 2) reaction conditions. In the presence of 10 mol% $\text{Co}_2(\text{CO})_8$ solutions of (trimethylsilyl)diazomethane in *n*-heptane are selectively carbonylated at 10 °C under an atmosphere of carbon monoxide to (trimethylsilyl)ketene in up to 80% isolated yield (reaction 1).



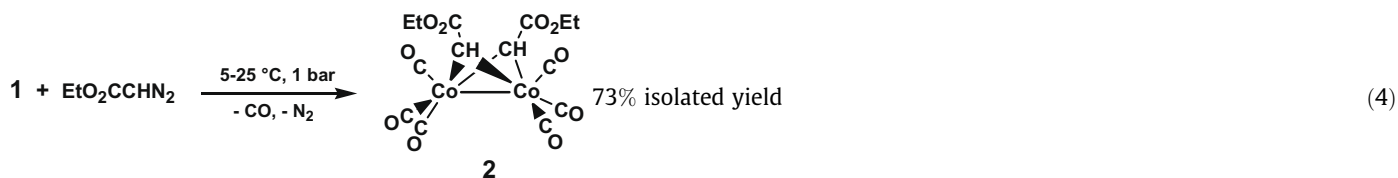
In the absence of external carbon monoxide the coordinated carbon monoxide ligands of octacarbonyl dicobalt are consumed in the (trimethylsilyl)ketene formation (reaction 2).



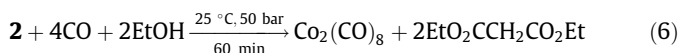
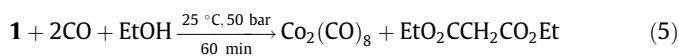
No intermediary cobalt complexes were detected by infrared spectroscopy in reactions 1 and 2. Ethyl diazoacetate behaves differently in the dediazotation reaction. At ambient conditions ethoxycarbonylcarbene-bridged dicobalt carbonyl complexes **1** and **2** were isolated from the reaction mixtures in good yields (reactions 3 and 4). Under an atmosphere of carbon monoxide the ethoxycarbonylcar-



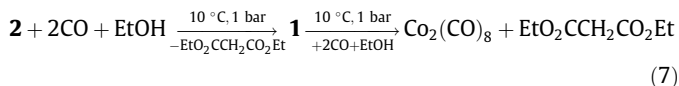
* Corresponding author. Tel.: +36 88 624 156; fax: +36 88 624 469.
E-mail address: ungvary@almos.vein.hu (F. Ungváry).



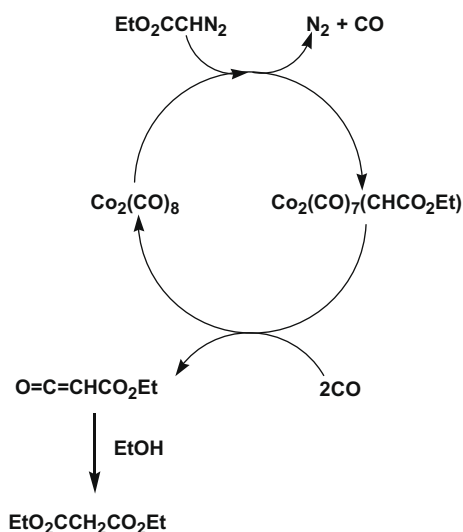
benzene ligand(s) of these complexes couple(s) with CO to give the highly reactive ethoxycarbonylketene, which can not be isolated but can be scavenged *in situ* by OH, NH, or CH acid compounds [2,3] or by *N*-substituted imines in a [2 + 2] cycloaddition reaction [4]. In the presence of ethanol both complexes **1** and **2** convert quantitatively to $\text{Co}_2(\text{CO})_8$ and diethyl malonate (reactions 5 and 6).



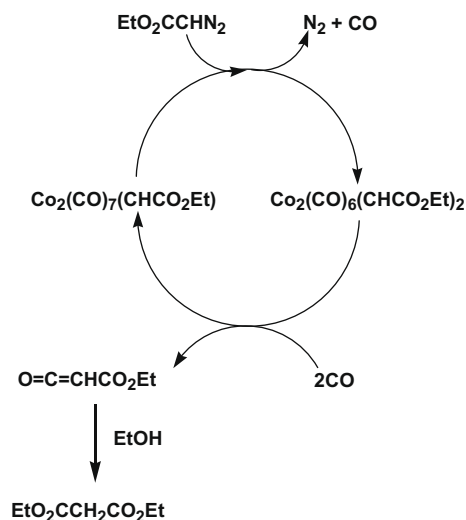
Experiments at atmospheric pressure of carbon monoxide have shown that complex **2** converts first rapidly to **1** and diethyl malonate, and in a much slower reaction complex **1** converts further to octacarbonyl dicobalt and to a second mol of diethyl malonate (Eq. (7)).



In both steps the formation of the highly reactive ethoxycarbonylketene was assumed by coupling of the ethoxycarbonylketene ligand with one of the coordinated carbon monoxide [2]. The combination of reactions 3–6 led to an effective one-pot procedure for the preparation of diethyl malonate by catalytic carbonylation of ethyl diazoacetate in the presence of a few mol% of octacarbonyl dicobalt [2]. Since diethyl malonate may be the product from both complex **1** and **2** two different catalytic cycles can be imagined depicted in Schemes 1 and 2.



Scheme 1.



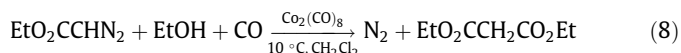
Scheme 2.

Triphenylphosphane- or $\text{Ph}_2\text{PCH}_2\text{PPh}_2$ -substituted derivatives of complex **1** were found to show similar catalytic activity in ethyl diazoacetate carbonylation as $\text{Co}_2(\text{CO})_8$, or complexes **1** or **2** [5–7].

In order to obtain a more detailed mechanism of the catalytic dediazotation and carbonylation of ethyl diazoacetate we investigated the kinetics of the catalytic reaction and the kinetics of the reactions in Schemes 1 and 2 at 10 °C in methylene chloride solutions.

2. Results

2.1. Experiments using $\text{Co}_2(\text{CO})_8$ as the catalyst precursor



The effect of the concentrations of $\text{Co}_2(\text{CO})_8$, ethyl diazoacetate, ethanol, and carbon monoxide on the rate of diethyl malonate formation in the catalytic carbonylation of ethyl diazoacetate (Eq. (8)) was studied in experiments performed between 1 and 100 bar pressure of carbon monoxide with various initial concentrations at 10 °C in CH_2Cl_2 solutions using 3 h reaction time (Table 1). The data in Table 1 show that under atmospheric pressure of carbon monoxide ($[\text{CO}] = 0.00507\text{--}0.00515\text{ mol/dm}^3$) the rate of diethyl malonate formation is practically linear with the initial concentrations of $\text{Co}_2(\text{CO})_8$ and that of ethyl diazoacetate, and independent of the ethanol concentrations (entries 1–15). The carbon monoxide concentration has a strong positive effect on the rate in the range between 0.005 and 0.03 mol/dm^3 (compare entries 1–15 with that of entries 16 and 17). On the other hand the carbon monoxide concentration has a little negative effect on the rate in the range between 0.44 and 1.12 mol/dm^3 (entries 29–33).

Table 1
The observed concentration of diethyl malonate [DEM]_{3h} and the observed rate of DEM formation ($r_{\text{DEM}} = [\text{DEM}]_{3\text{h}}/3 \times 3600$ in the catalytic carbonylation reaction of ethyl diazoacetate (EDA) at 10 °C under CO in 3 h reaction time applying $\text{Co}_2(\text{CO})_8$ as the catalyst precursor in the presence of ethanol using various initial concentrations of the reactants.

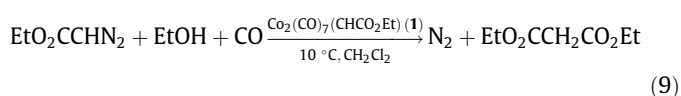
Entry	$10^2 \times [\text{CO}]_0^a$ (mol/dm ³)	$[\text{Co}_2(\text{CO})_8]_0$ (mol/dm ³)	$[\text{EDA}]_0$ (mol/dm ³)	$[\text{Ethanol}]_0$ (mol/dm ³)	$[\text{DEM}]_{3\text{h}}^b$ (mol/dm ³)	$10^5 \times r_{\text{DEM}}$ (mol/dm ³ s)	$[\text{EDA}]_0/[\text{CO}]_0$
1	0.512	0.005	0.010	0.05	0.00135	0.0125	1.95
2	0.509	0.005	0.020	0.05	0.00256	0.0237	3.93
3	0.512	0.005	0.050	0.05	0.00820	0.0759	9.77
4	0.512	0.005	0.100	0.05	0.01651	0.1529	19.53
5	0.508	0.0125	0.250	0.25	0.0138	0.128	49.21
6	0.512	0.025	0.250	0.25	0.0276	0.256	48.83
7	0.507	0.050	0.125	0.25	0.0299	0.277	24.65
8	0.510	0.050	0.125	0.25	0.0275	0.255	24.51
9	0.508	0.050	0.250	0.125	0.0552	0.511	49.21
10	0.515	0.050	0.250	0.25	0.0529	0.490	48.54
11	0.512	0.100	0.250	0.25	0.0989	0.916	48.83
12	0.508	0.050	0.250	0.50	0.0522	0.511	49.21
13	0.507	0.050	0.500	0.25	0.1150	1.065	98.62
14	0.510	0.050	0.500	0.25	0.1173	1.086	98.04
15	0.510	0.025	0.500	0.50	0.0582	0.493	98.04
16	1.02	0.025	0.500	0.50	0.088	0.820	49.02
17	2.80	0.025	0.500	0.50	0.130	1.20	17.86
18	7.27	0.025	0.500	0.50	0.134	1.24	6.88
19	14.76	0.025	0.500	0.50	0.140	1.30	3.39
20	22.24	0.025	0.500	0.50	0.169	1.56	2.25
21	29.73	0.025	0.500	0.50	0.184	1.70	1.68
22	37.22	0.005	0.010	0.05	0.0020	0.0185	0.027
23	37.22	0.005	0.020	0.05	0.0045	0.0417	0.054
24	37.22	0.005	0.100	0.05	0.0083	0.077	0.269
25	37.22	0.025	0.500	0.50	0.207	1.92	1.340
26	37.22	0.025	0.250	0.25	0.087	0.889	0.67
27	37.22	0.025	0.125	0.25	0.052	0.482	0.336
28	37.22	0.025	0.050	0.25	0.022	0.204	0.134
29	44.71	0.025	0.500	0.50	0.212	1.96	1.12
30	59.69	0.025	0.500	0.50	0.171	1.58	0.84
31	74.66	0.025	0.500	0.50	0.134	1.24	0.672
32	112.11	0.025	0.500	0.50	0.111	1.03	0.446
33	112.11	0.005	0.05	0.02	0.0067	0.062	0.0446
34	112.11	0.005	0.01	0.01	0.0019	0.017	0.0089

^a Calculated from the partial pressure of CO and the known solubility of CO in CH_2Cl_2 expressed in mol fraction: x_{CO} (10 °C, 1 bar of $P(\text{CO}) = 0.000473$ converted to $[\text{CO}] = 0.007489$ mol/dm³ (see Refs. [9,10]).

^b Determined by quantitative infrared spectroscopy.

The composition of the cobalt complexes in the reaction mixture checked by infrared spectroscopy after 3 h of reaction time shows the presence of three different cobalt complexes: $\text{Co}_2(\text{CO})_8$, $\text{Co}_2(\text{CO})_7(\text{CHCO}_2\text{Et})$ (**1**), and $\text{Co}_2(\text{CO})_6(\text{CHCO}_2\text{Et})_2$ (**2**) which can be recognized in the mixtures by their characteristic $\nu(\text{CO})$ bands at 2022, 2075 and 2080 cm^{-1} , respectively. The composition depends basically on the applied CO pressure and on the $[\text{EDA}]/[\text{CO}]$ concentration ratio in the experiment. Thus, at 1 bar CO pressure using $[\text{EDA}]/[\text{CO}] = 1.95$ (entry 1) the cobalt composition is in form of >16% complex **2**, 80% complex **1**, and <4% $\text{Co}_2(\text{CO})_8$. If the $[\text{EDA}]/[\text{CO}]$ ratio is 10-fold higher, 19.53 (entry 4), the cobalt composition is in form of <64% complex **2**, 16% complex **1**, and 0% $\text{Co}_2(\text{CO})_8$. Interestingly in this experiment and even more pronounced in those performed at higher $[\text{EDA}]/[\text{CO}]$ ratios (entries 5, 6, 10, and 11), in addition of the $\nu(\text{CO})$ bands of the known complexes a shoulder appears at 2060 cm^{-1} . At 50 bar CO pressure using $[\text{EDA}]/[\text{CO}] = 1.34$ (entry 25) the cobalt composition is in form of 16% complex **2**, 56% complex **1**, and 28% $\text{Co}_2(\text{CO})_8$. If the $[\text{EDA}]/[\text{CO}]$ ratio is 50-fold lower, 0.027 (entry 22), >95% of the cobalt is in form of $\text{Co}_2(\text{CO})_8$. The amounts of complex **1** and complex **2** in this case could not be determined from the infrared spectra.

2.2. Experiments using $\text{Co}_2(\text{CO})_7(\text{CHCO}_2\text{Et})$ (**1**) as the catalyst precursor



The effect of the concentrations of complex **1**, ethyl diazoacetate, and ethanol on the rate of diethyl malonate formation in the catalytic carbonylation of ethyl diazoacetate (Eq. (9)) was studied in experiments performed under atmospheric pressure of carbon monoxide with various initial concentrations at 10 °C in CH_2Cl_2 solutions using various reaction times (Table 2). The data in Table 2 show that the rate of diethyl malonate formation is first order with respect to complex **1**, less than first order in ethyl diazoacetate, and independent of the ethanol concentrations. The composition of the cobalt complexes in the reaction mixture checked by infrared spectroscopy shows the presence of mainly complex **1**, and less of complex **2**, which can be recognized in the mixtures by their characteristic $\nu(\text{CO})$ bands at 2075 and 2080 cm^{-1} , respectively. Higher concentration of ethyl diazoacetate influences not only the rate of reaction 9, but results in a little higher ratio of **2**/**1**. This latter finding arouses the suspicion that the effect of ethyl diazoacetate on the rate works by the formation of the much more active complex **2**. Results of experiments using $\text{Co}_2(\text{CO})_6(\text{CHCO}_2\text{Et})_2$ (**2**) as the catalyst precursor (see Section 2.3) support this suspicion.

2.3. Experiments using $\text{Co}_2(\text{CO})_6(\text{CHCO}_2\text{Et})_2$ (**2**) as the catalyst precursor

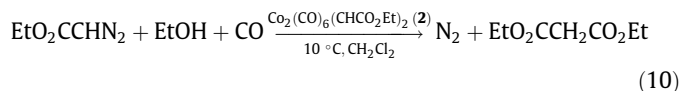


Table 2

The observed concentration of diethyl malonate [DEM]_t, the observed rate of DEM formation ($r_{\text{DEM}}^1 = [\text{DEM}]_t / t \times 60$), and the calculated observed rate constant $k_{\text{DEM}}^1 = r_{\text{DEM}}^1 / [\text{Co}_2(\text{CO})_7(\text{CHCO}_2\text{Et})]_0 \times [\text{EDA}]_0$ in the $\text{Co}_2(\text{CO})_7(\text{CHCO}_2\text{Et})$ (**1**)-catalyzed carbonylation reaction of ethyl diazoacetate (EDA) at 10 °C under atmospheric pressure of CO in the presence of ethanol using various initial concentrations of the reactants.

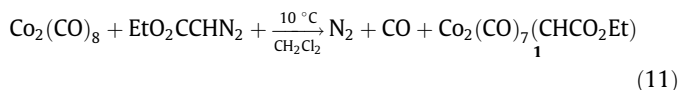
Entry	$10^2 \times [\text{CO}]_0^a$ (mol/dm ³)	$[\mathbf{1}]_0$ (mol/dm ³)	$[\text{EDA}]_0$ (mol/dm ³)	$[\text{Ethanol}]_0$ (mol/dm ³)	t Time (Min)	$[\text{DEM}]_t^b$ (mol/dm ³)	$[\mathbf{1}]_t$ (mol/dm ³)	$10^5 \times r_{\text{DEM}}^1$ (mol/dm ³ s)	$10^5 \times k_{\text{DEM}}^1$ (dm ³ /mol s)
1	0.518	0.005	0.01	0.043	252	0.0018	0.0037	0.0118	235
2	0.500	0.010	0.01	0.02	180	0.0025	0.0083	0.0232	232
3	0.521	0.010	0.01	0.04	216	0.0029	0.0073	0.0224	224
4	0.500	0.010	0.02	0.02	150	0.0032	0.0069	0.0342	171
5	0.500	0.010	0.04	0.02	180	0.0044	0.0060	0.0407	102

^a Calculated from the partial pressure of CO and the known solubility of CO in CH_2Cl_2 (see Refs. [9,10]).

^b Determined by quantitative infrared spectroscopy.

The effect of the concentrations of complex **2**, ethyl diazoacetate, and ethanol on the rate of diethyl malonate formation in the catalytic carbonylation of ethyl diazoacetate (Eq. (10)) was studied in experiments performed between 1 and 3.4 bar pressure of carbon monoxide with various initial concentrations at 10 °C in CH_2Cl_2 solutions (Table 3). The rates in Table 3 are one order of magnitude higher than those in Table 2. The data in Table 3 show that the rate of diethyl malonate formation is first order with respect to complex **2**, and independent of the concentrations of ethyl diazoacetate, and that of ethanol. During the catalytic reaction 7–30% of complex **2** converts to complex **1**.

2.4. The reaction of $\text{Co}_2(\text{CO})_8$ with $\text{EtO}_2\text{CCHN}_2$



The kinetics of the reaction of $\text{Co}_2(\text{CO})_8$ with ethyl diazoacetate (Eq. (11)) has been studied earlier in *n*-heptane solution by measuring the initial rate of gas evolution and by measuring the initial rate of the decrease of the $\text{Co}_2(\text{CO})_8$ concentration at various initial concentrations of $\text{Co}_2(\text{CO})_8$, $\text{EtO}_2\text{CCHN}_2$ and CO at 10 °C [8]. The observed kinetics was found to be in accord with a reversible dissociation of carbon monoxide from $\text{Co}_2(\text{CO})_8$, followed by a reaction with ethyl diazoacetate (Scheme 3).

Assuming steady-state concentration for the $\text{Co}_2(\text{CO})_7$ intermediate, the rate could be described by Eq. (12) or after rearrangement by Eq. (13).

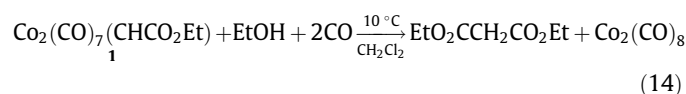
$$r = k_2[\text{Co}_2(\text{CO})_7][\text{EtO}_2\text{CCHN}_2] = \frac{k_1 k_2 [\text{Co}_2(\text{CO})_7][\text{EtO}_2\text{CCHN}_2]}{k_{-1}[\text{CO}] + k_2[\text{EtO}_2\text{CCHN}_2]} \quad (12)$$

$$\frac{[\text{Co}_2(\text{CO})_8]}{r} = \frac{k_{-1}}{k_1 k_2} \frac{[\text{CO}]}{[\text{EtO}_2\text{CCHN}_2]} + \frac{1}{k_1} \quad (13)$$

A plot of $[\text{Co}_2(\text{CO})_8]/r$ against $[\text{CO}]/[\text{EtO}_2\text{CCHN}_2]$ using the experimental initial concentrations and the observed initial rates allowed the calculation of k_1 (10 °C, *n*-heptane) = $(1.22 \pm 0.06) \times 10^{-3} \text{ s}^{-1}$ and the ratio of k_{-1}/k_2 (10 °C, *n*-heptane) = 1.34 ± 0.07 from the intercept and the slope, respectively.

In order to have all kinetic information of the steps of Schemes 1 and 2 measured in CH_2Cl_2 solution we repeated the kinetic investigation of reaction 11 in CH_2Cl_2 as well. The results showed the same kinetic patterns. A plot of $[\text{Co}_2(\text{CO})_8]/r_{\text{in}}$ against $[\text{CO}]/[\text{EtO}_2\text{CCHN}_2]$ using the experimental initial concentrations and the observed initial rates (r_{in}) in Table 4 allowed the calculation of k_1 (10 °C) = $(0.42 \pm 0.03) \times 10^{-3} \text{ s}^{-1}$ and the ratio of k_{-1}/k_2 (10 °C) = 7.6 ± 0.2 from the intercept and the slope, respectively (see Fig. 1). Thus, in CH_2Cl_2 the dissociation of a CO ligand from $\text{Co}_2(\text{CO})_8$ is 0.344-times slower than in *n*-heptane. The 5.7-times higher ratio of k_{-1}/k_2 in CH_2Cl_2 indicate a strong solvent effect for the ratio of the competing reactions as well.

2.5. The reaction of $\text{Co}_2(\text{CO})_7(\text{CHCO}_2\text{Et})$ (**1**) with CO and EtOH

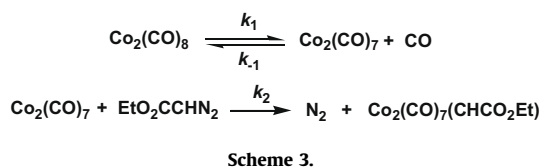
**Table 3**

The observed concentration of diethyl malonate [DEM]_t, the observed rate of DEM formation ($r_{\text{DEM}}^2 = [\text{DEM}]_t / t \times 60$), and the calculated rate constant $k_{\text{DEM}}^2 = r_{\text{DEM}}^2 / [\text{Co}_2(\text{CO})_6(\text{CHCO}_2\text{Et})_2]_0 \times [\text{CO}]_0$ in the $\text{Co}_2(\text{CO})_6(\text{CHCO}_2\text{Et})_2$ (**2**)-catalyzed carbonylation reaction of ethyl diazoacetate (EDA) at 10 °C under CO in the presence of ethanol using various initial concentrations of the reactants.

Entry	$10^2 \times [\text{CO}]_0^a$ (mol/dm ³)	$10^2 \times [\mathbf{2}]_0$ (mol/dm ³)	$[\text{EDA}]_0$ (mol/dm ³)	$[\text{Ethanol}]_0$ (mol/dm ³)	t Time (Min)	$10^2 \times [\text{DEM}]_t^b$ (mol/dm ³)	$10^2 \times [\mathbf{1}]_t$ (mol/dm ³)	$10^5 \times r_{\text{DEM}}^2$ (mol/dm ³ s)	$10^5 \times k_{\text{DEM}}^2$ (dm ³ /mol s)
1	0.499	0.50	0.010	0.05	60	0.164	0.128	0.0456	1830
2	0.503	0.50	0.025	0.05	60	0.166	0.113	0.0460	1829
3	0.504	0.50	0.050	0.05	60	0.152	0.089	0.0422	1675
4	0.504	0.50	0.050	0.05	90	0.230	0.101	0.0426	1690
5	0.504	0.50	0.050	0.05	120	0.305	0.103	0.0423	1679
6	0.510	0.50	0.100	0.05	90	0.234	0.051	0.0433	1697
7	0.510	0.50	0.100	0.05	125	0.322	0.049	0.0447	1752
8	0.510	1.00	0.010	0.05	30	0.152	0.167	0.0843	1651
9	0.510	1.00	0.010	0.05	60	0.299	0.250	0.0831	1629
10	0.510	1.00	0.010	0.40	60	0.306	0.265	0.0850	1665
11	1.478	0.50	0.050	0.02	15	0.087	0.082	0.0966	1308
12	2.370	0.50	0.050	0.02	15	0.106	0.104	0.1181	997
13	2.355	0.50	0.100	0.05	30	0.204	0.151	0.1130	960
14	2.335	0.50	0.500	0.25	75	0.469	0.025	0.1042	893

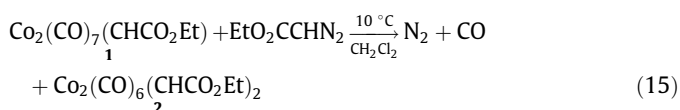
^a Calculated from the partial pressure of CO and the known solubility of CO in CH_2Cl_2 (see Refs. [9,10]).

^b Determined by quantitative infrared spectroscopy.



In the presence of ethanol the ethoxycarbonylcarbene-bridged complex $\text{Co}_2(\text{CO})_7(\text{CHCO}_2\text{Et})$ (**1**) reacts with CO according to Eq. (14) to give diethyl malonate and $\text{Co}_2(\text{CO})_8$. The rate of the reaction was followed by measuring the increase of the diethyl malonate concentration versus reaction time using quantitative infrared spectroscopy. The data in Table 5 show that the rate of diethyl malonate formation is first order with respect to both the complex and the CO concentration, and zero order with respect to the ethanol concentration. Accordingly the rate constant of the reaction was calculated as $k_{\text{DEM}}^1(10^\circ\text{C}) = r_{\text{DEM}}^1/[\mathbf{1}][\text{CO}] = (40 \pm 5) \times 10^{-5} \text{ dm}^3/\text{mol s}$. The observed first order in complex **1** and carbon monoxide concentration suggests that the rate-determining step involves 1 mol of complex **1** and 1 mol of external carbon monoxide. The rate-determining reaction might involve the synchronous coordination of an external carbon monoxide and the coupling of the ethoxycarbonylcarbene ligand with one of the coordinated CO ligands. The subsequent formation of $\text{Co}_2(\text{CO})_8$ and ethoxycarbonylketene involves the fast coordination of a second mol of external carbon monoxide. The independency of the rate from the ethanol concentration supports the assumption that the final diethyl malonate formation is also a fast reaction between ethanol and the intermediate ethoxycarbonylketene. It is remarkable that under atmospheric pressure reaction 14 takes place twice as fast in the absence of carbon monoxide (entry 4 in Table 5). Source of carbon monoxide in this case may be the partial decomposition of the carbonyl cobalt complexes in the reaction mixture.

2.6. The reaction of $\text{Co}_2(\text{CO})_7(\text{CHCO}_2\text{Et})$ (**1**) with $\text{EtO}_2\text{CCHN}_2$



Complex **1** also is an effective dediazotation reagent for ethyl diazoacetate. Products of the dediazotation reaction are N_2 , CO, and complex **2** according to reaction 15. It takes only a few minutes to achieve a complete conversion if the CO formed in the reaction is continuously swept away by argon. We studied the kinetics of the

Table 4

The effect of concentrations of $\text{Co}_2(\text{CO})_8$ and ethyl diazoacetate on the initial rate (r_{in}) of the reaction: $\text{Co}_2(\text{CO})_8 + \text{N}_2\text{CHCO}_2\text{Et} \rightarrow \text{Co}_2(\text{CO})_7(\text{CHCO}_2\text{Et}) + \text{CO} + \text{N}_2$ under atmospheric pressure (740–750 mmHg) of carbon monoxide in CH_2Cl_2 solution at 10°C .

$[\text{Co}_2(\text{CO})_8]_0$ (mol/dm ³)	$[\text{EDA}]_0$ (mol/dm ³)	$[\text{CO}]_0^a$ (mol/dm ³)	$10^5 \times r_{\text{in}}$ (mol/dm ³ s)	$[\text{Co}_2(\text{CO})_8]_0/r_{\text{in}}$ (s)	$[\text{CO}]_0/[\text{N}_2\text{CHCO}_2\text{Et}]_0$
0.01	0.04	0.00506	0.634	1577	0.126
0.01	0.02	0.00506	0.418	2392	0.253
0.01	0.01	0.00506	0.295	3396	0.506
0.02	0.01	0.00507	0.579	3454	0.507
0.04	0.01	0.00510	1.275	3137	0.510
0.01	0.005	0.00506	0.174	5744	1.013
0.01	0.00333	0.00508	0.1225	8165	1.527
0.01	0.00333	0.00509	0.1226	8156	1.528
0.01	0.0025	0.00508	0.0952	10504	2.034
0.01	0.0020	0.00498	0.0809	12361	2.488
0.01	0.00166	0.00510	0.0691	14461	3.075
0.01	0.00125	0.00510	0.0623	16051	3.496

^a Calculated from the partial pressure of CO and the known solubility of CO in CH_2Cl_2 (see Refs. [9,10]).

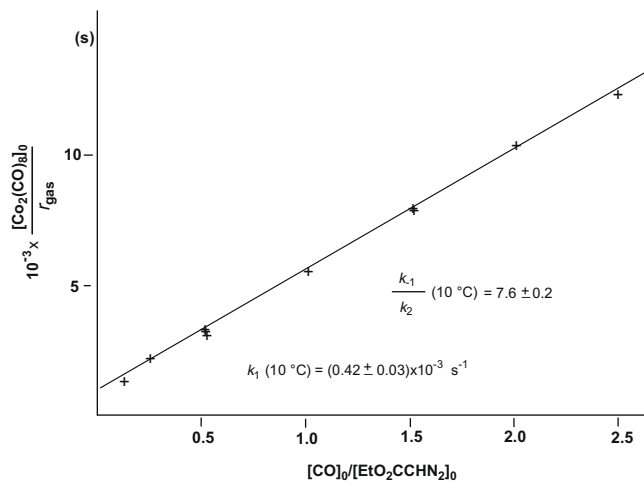


Fig. 1. Plot of the observed initial gas evolution rates (r_{gas}) in the reaction: $\text{Co}_2(\text{CO})_8 + \text{EtO}_2\text{CCHN}_2 \rightarrow \text{Co}_2(\text{CO})_7(\text{CHCO}_2\text{Et}) + \text{N}_2 + \text{CO}$ in CH_2Cl_2 solution at 10°C at various initial concentrations according to Eq. (13).

reaction by measuring the initial rate of gas evolution (r_{gas}^1) and by measuring the initial rate of the decrease of the $\text{Co}_2(\text{CO})_7(\text{CHCO}_2\text{Et})$ (**1**) concentration ($r_{-[\mathbf{1}]}^1$) at various initial concentrations of complex **1**, $\text{EtO}_2\text{CCHN}_2$ and CO at 10°C in CH_2Cl_2 solution. The decrease of the $\text{Co}_2(\text{CO})_7(\text{CHCO}_2\text{Et})$ concentration was followed by the decrease of intensity of the well separated bridging $\nu(\text{C}=\text{O})$ band of complex **1** at 1853 cm^{-1} . In experiments started under an atmosphere of argon we found a linear dependence of the observed rates on the initial concentrations of complex **1** (see Fig. 2).

Raising the initial concentrations of $\text{EtO}_2\text{CCHN}_2$ has a positive effect on the observed rates. On the other hand the presence of CO in the gas atmosphere has a negative effect on the rate of the dediazotation reaction. This kinetic behavior is in accordance with a reversible dissociation of CO from complex **1**, followed by a reaction with $\text{EtO}_2\text{CCHN}_2$ (Scheme 4).

Assuming steady-state concentration for the $\text{Co}_2(\text{CO})_6(\text{CHCO}_2\text{Et})$ intermediate, the rate can be described by Eq. (16) or after rearrangement by Eq. (17).

$$\begin{aligned} r_{-[\mathbf{1}]}^1 &= k_{-1}^1 [\text{Co}_2(\text{CO})_6(\text{CHCO}_2\text{Et})] [\text{EtO}_2\text{CCHN}_2] \\ &= \frac{k_1^1 k_2^1 [\text{Co}_2(\text{CO})_7(\text{CHCO}_2\text{Et})] [\text{EtO}_2\text{CCHN}_2]}{k_{-1}^1 [\text{CO}] + k_2^1 [\text{EtO}_2\text{CCHN}_2]} \end{aligned} \quad (16)$$

$$\frac{[\text{Co}_2(\text{CO})_7(\text{CHCO}_2\text{Et})]}{r_{-[\mathbf{1}]}^1} = \frac{k_{-1}^1}{k_1^1 k_2^1} \frac{[\text{CO}]}{[\text{EtO}_2\text{CCHN}_2]} + \frac{1}{k_1^1} \quad (17)$$

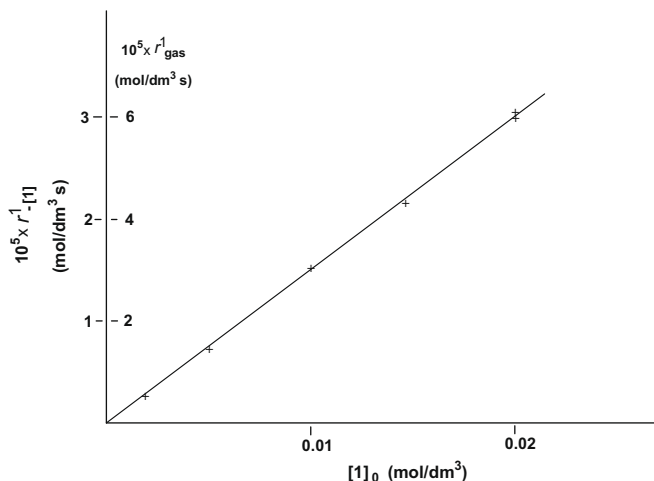
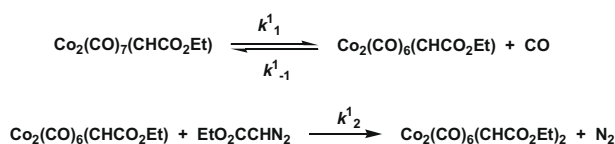


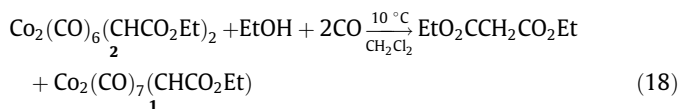
Fig. 2. Plot of the observed initial gas evolution rates (r_{gas}^1) and initial disappearance rates of complex **1** (r_{-1}^1) in the reaction: $\text{Co}_2(\text{CO})_7(\text{CHCO}_2\text{Et}) + \text{EtO}_2\text{CCHN}_2 \rightarrow \text{Co}_2(\text{CO})_6(\text{CHCO}_2\text{Et})_2 + \text{N}_2 + \text{CO}$ in CH_2Cl_2 solution started under an atmosphere of argon at 10°C at $[\text{EtO}_2\text{CCHN}_2]_0 = 0.010 \text{ mol/dm}^3$ at various initial concentrations of complex **1**.



Scheme 4.

A plot of $[\mathbf{1}]/r_{-1}^1$ against $[\text{CO}]/[\text{EtO}_2\text{CCHN}_2]$ using the experimental initial concentrations and the observed initial rates allowed the calculation of k_1^1 (10°C) = $(15 \pm 5) \times 10^{-3} \text{ s}^{-1}$ and the ratio of k_1^1/k_2^1 (10°C) = 410 ± 140 from the intercept and the slope, respectively (see Fig. 3). A comparison of k_1^1 with k_1 shows that the formation of the coordinatively unsaturated intermediate $\text{Co}_2(\text{CO})_6(\text{CHCO}_2\text{Et})$ from complex **1** is more than 35-times faster than that of $\text{Co}_2(\text{CO})_7$ from $\text{Co}_2(\text{CO})_8$. Despite of this difference the overall rate of the reaction of ethyl diazoacetate with $\text{Co}_2(\text{CO})_8$ ($k_1 k_2/k_{-1} = 5.53 \times 10^{-5} \text{ s}^{-1}$) is only 1.52-times faster than that with complex **1** ($k_1^1 k_2^1/k_{-1}^1 = 3.65 \times 10^{-5} \text{ s}^{-1}$).

2.7. The reaction of $\text{Co}_2(\text{CO})_6(\text{CHCO}_2\text{Et})_2$ (**2**) with CO and EtOH



In the presence of ethanol the ethoxycarbonylcarbene-bridged complex $\text{Co}_2(\text{CO})_6(\text{CHCO}_2\text{Et})_2$ (**2**) reacts with CO according to Eq. (18) to give diethyl malonate and $\text{Co}_2(\text{CO})_7(\text{CHCO}_2\text{Et})$ (**1**) in the first step. The rate of the reaction was followed by measuring the increase of the diethyl malonate concentration versus reaction time using quantitative infrared spectroscopy. The data in Table 6 show that the rate of diethyl malonate formation is first order with respect to both the complex and the CO concentration, and zero order with respect to the ethanol concentration. In a few cases the rates of the reaction were calculated based on the amount of complex **1** formed in the reaction (see for example entry 2), and based on the amount of CO absorbed in the reaction (see for example entry 3) in good agreement with the rates calculated on the basis of the amount of diethyl malonate formed in the reaction.

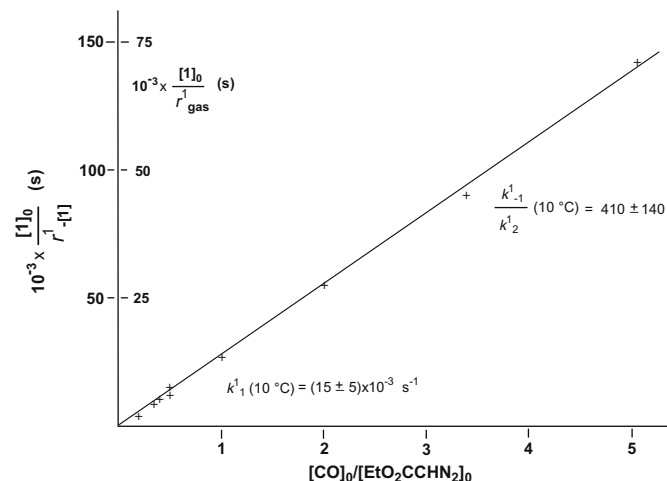
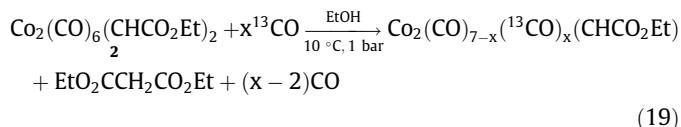


Fig. 3. Plot of the observed initial gas evolution rates (r_{gas}^1) and initial disappearance rates of complex **1** (r_{-1}^1) in the reaction: $\text{Co}_2(\text{CO})_7(\text{CHCO}_2\text{Et}) + \text{EtO}_2\text{CCHN}_2 \rightarrow \text{Co}_2(\text{CO})_6(\text{CHCO}_2\text{Et})_2 + \text{N}_2 + \text{CO}$ in CH_2Cl_2 solution at 10°C at various initial concentrations according to Eq. (17).

Accordingly the rate constant of the reaction was calculated as k_{DEM}^2 (10°C) = $r_{\text{DEM}}^2/[\mathbf{2}][\text{CO}] = (2640 \pm 220) \times 10^{-5} \text{ dm}^3/\text{mol s}$, which is 67.5-times faster than the analogous reaction with complex **1**. The observed first order in complex **2** and carbon monoxide concentration suggests that the rate-determining step involves one mol of complex **2** and 1 mol of carbon monoxide, which might be the coordination of an external carbon monoxide synchronously to the coupling of the ethoxycarbonylcarbene ligand with one of the coordinated CO ligands. The subsequent fast formation of complex **1** and free ethoxycarbonylketene involves the coordination of a second mol of carbon monoxide. The independency of the rate from the ethanol concentration supports the assumption that the final diethyl malonate formation is also a fast reaction between ethanol and the intermediate ethoxycarbonylketene. These assumptions were verified by the fact that reaction of complex **2** with ^{13}CO in the presence of excess ethanol (reaction 19) results in diethyl malonate with natural isotopic distribution of ^{13}C [11].



If a solution of complex **2** and ethanol was kept under the same conditions but under an atmosphere of argon instead of carbon monoxide, 20-times slower formation of diethyl malonate could be observed parallel to the decrease of the concentration of complex **2** (see entries 4 and 5, respectively). The much slower formation of diethyl malonate suggests that the coupling of the ethoxycarbonylcarbene ligand with one of the coordinated CO ligands might occur in a small extent even in the absence of the beneficial external carbon monoxide, and the ethoxycarbonylketene product is successfully trapped by the ethanol present. Source of carbon monoxide in this case may be the partial decomposition of the carbonyl cobalt complexes in the reaction mixture.

The experimentally determined rate constants of the assumed steps in the cobalt–carbonyl catalyzed carbonylation of ethyl diazoacetate at 10°C in CH_2Cl_2 solution have been compiled in Scheme 5.

2.8. Computational studies on the ketene formation step

In order to get deeper insights into the mechanism of the ketene formation from the bridged carbene complex **1** the ketene forma-

tion and the ketene elimination elementary steps were studied by means of density functional calculations using the BP86 functional which gives usually a reasonable prediction for carbonyl vibrational frequencies [12]. More detailed computational investigations on the cobalt-catalyzed ketene formation reaction comprising all elementary steps are underway.

Isomers of **1** were described thoroughly in one of our previous papers [13]. It was reported that the arrangement of the H–C–C=O is anti-periplanar as its energy is by 2.1 kcal/mol lower than

that of the syn-periplanar isomer. The energy difference of both conformers was recomputed at the BP86 level of theory and was found to be 2.5 kcal/mol. The relative stability of anti-periplanar and syn-periplanar conformations of the species occurring in this computational study has also been checked and the former one was proved to be slightly more stable in all cases.

The structure of **1** computed at the BP86 level reveals symmetry very close to C_s . It was shown previously [13] that this species tend to release one CO with a relatively small free energy of dissociation-

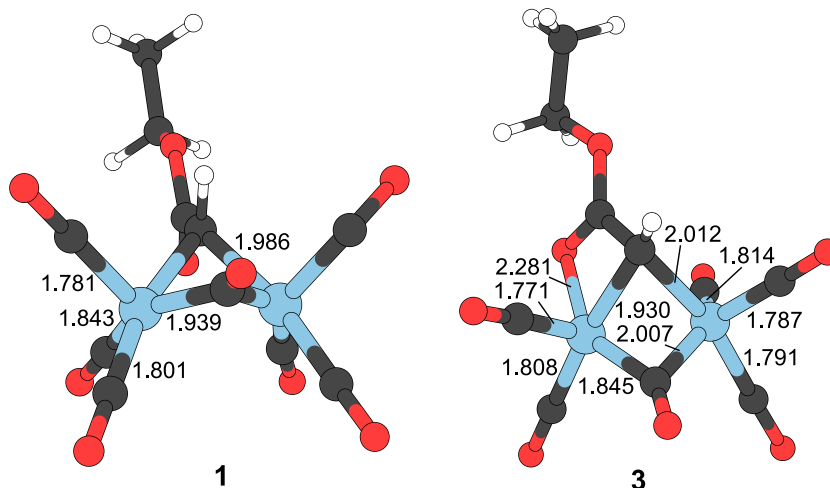


Fig. 4. Computed structure of **1** and its coordinative unsaturated derivative **3** formed by dissociation of one CO. Bond distances are given in Å.

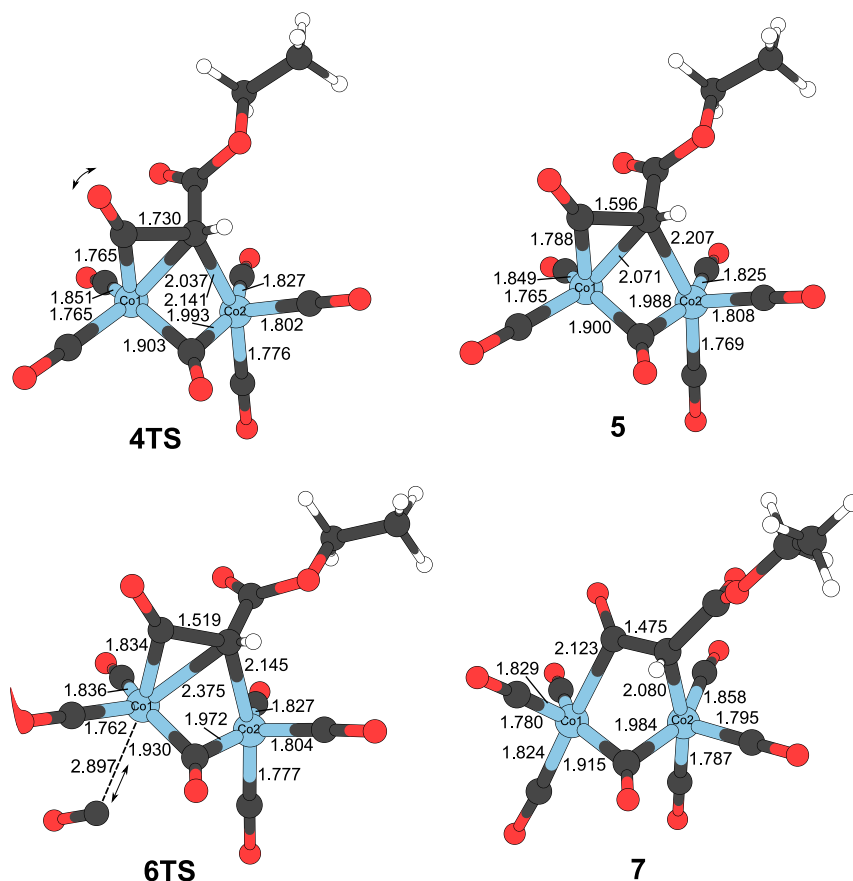


Fig. 5. Computed structures of the transition state for the intramolecular ketene formation (**4TS**), the coordinative unsaturated ketene complex (**5**), the transition state for the coordination of an additional CO (**6TS**) and the coordinative saturated ketene complex (**7**). Bond distances are given in Å.

tion. The predicted ΔG for the reaction $1 \rightarrow 3 + \text{CO}$ is 9.3 kcal/mol, slightly higher than that obtained at the B3LYP level (6.9 kcal/mol). The geometry parameters computed with the two functionals are in close agreement except the distance between the carbonyl oxygen of the ethoxycarbonyl ligand and the interacting cobalt, which is somewhat higher at the BP86 level suggesting a slightly weaker computed interaction. The structure of complexes **1** and **3** are depicted in Fig. 4. Their characteristic $\nu(\text{CO})$ bands are computed to be at 2054 and 2041 cm^{-1} , respectively.

The CH moiety belonging to the bridging carbene group is found to couple with one of the axial terminal carbonyl ligands resulting in ketene complex **5**, which has a computed characteristic $\nu(\text{CO})$ band at 2045 cm^{-1} . The intramolecular carbene–CO coupling pro-

ceeds in a fast reaction as the free energy of activation is only 8.9 kcal/mol whereas the reaction free energy is 8.5 kcal/mol, thus endothermic. The transition state **4TS** related to the formation of the ketene complex has a single imaginary frequency of 185i cm^{-1} . The ketene complex **5** is an interesting intermediate example between the $(\mu^1-\eta^2)$ and $(\mu^2-\eta^2)$ coordination modes as the CH moiety is bound stronger to Co1, however the strength of the interaction to Co2 is not negligible, suggested by the 2.207 Å C–Co bond length (see Fig. 5). The coordinative unsaturated complex **5** takes up one external carbon monoxide resulting in the saturated species **7** via transition state **6TS**, which has a characteristic imaginary frequency of 122i cm^{-1} . Unlike **5**, complex **7** can be characterized as a true $(\mu^2-\eta^2)$ ketene complex with a computed

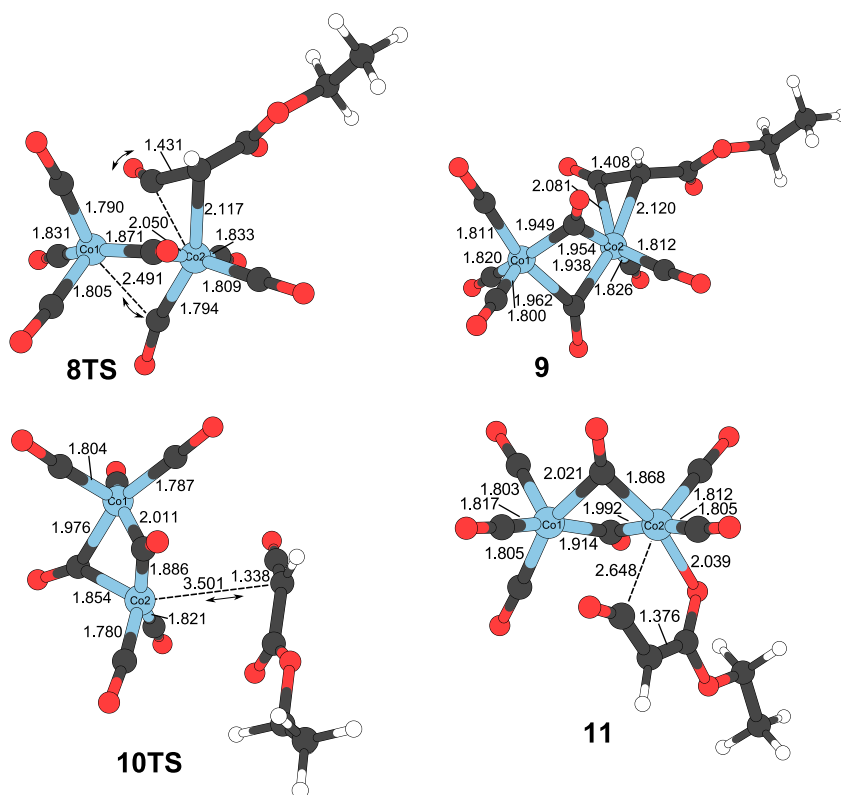


Fig. 6. Computed structures of the transition state for the interconversion of the coordinative saturated ketene complex (**8TS**), the coordinative saturated $(\mu^1-\eta^2)$ ketene complex (**9**), the transition state for the dissociation of ethoxycarbonylketene (**10TS**) and the reformed ketene complex (**11**) bounding ketene via its carbonyl oxygen. Bond distances are given in Å.

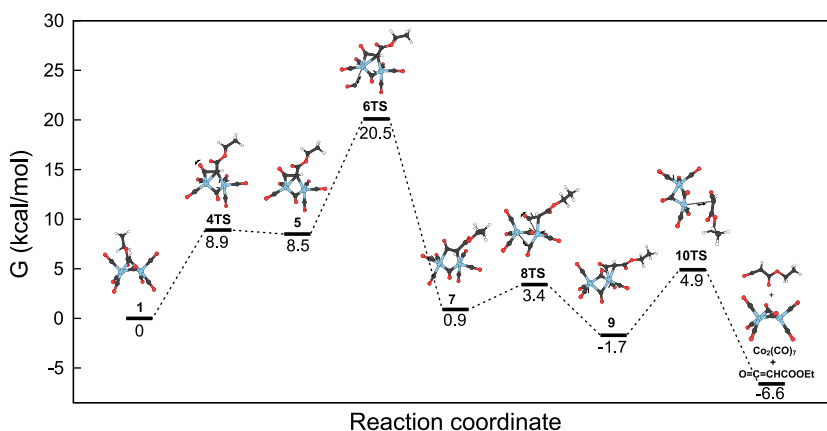


Fig. 7. Proposed free energy profile of the ketene formation and dissociation pathway.

Table 7

Charge Decomposition Analysis (CDA) of complexes **7**, **9**, and **11**. Interaction energy values are given in kcal/mol.

	7	9	11
Donation (d)	0.515e	0.590e	0.645e
Back-donation (b)	0.099e	0.278e	0.200e
Repulsive polarization (r)	-0.242e	-0.180e	-0.159e
Residual term (Δ)	0.091e	-0.037e	-0.020e
Interaction energy	-81.64	-38.64	-39.14

characteristic $\nu(\text{CO})$ band at 2052 cm^{-1} . The coordination of CO is almost isoenergetic as the free energy of the reaction is 0.9 kcal/mol .

It is predicted that the coordination mode of **7** is not the most stable one as it is prone to form **9** in a very facile rearrangement via a free energy barrier of 2.6 kcal/mol . The transition state related to the interconversion is designated as **8TS**, having a single imaginary frequency of $76i\text{ cm}^{-1}$, is featured by a simultaneous migration of the ketene ligand from Co1 to Co2 and the decrease of the Co1–Co2–C angle of one of the terminal CO ligand leading to a ketene complex possessing to bridging carbonyl ligands (see Fig. 6). The $(\mu^1-\eta^2)$ complex **9** is by 2.5 kcal/mol more stable in term of free energy than **7** with characteristic $\nu(\text{CO})$ bands at 2031 cm^{-1} and 1863 cm^{-1} related to the harmonic vibrations of terminal and bridging carbonyls, respectively.

The coordinated ketene ligand dissociates from **9** via a small free energy barrier of 6.6 kcal/mol suggesting that ketene complexes formed by the coupling of the bridging carbene and one terminal CO ligands cannot be observed experimentally by IR spectroscopy; they provide readily free ketene instead. The ketene dissociation step is exothermic in term of free energy by -5.5 kcal/mol . The transition state **10TS** has a single imaginary frequency of $73i\text{ cm}^{-1}$. Intrinsic reaction coordinate (IRC) calculation revealed that **10TS** indeed connects **9** and the dissociated ketene along with the dibridged $\text{Co}_2(\text{CO})_7$ complex. Similar homoleptic dirhodium heptacarbonyl complex is described recently [14], but to the best of our knowledge dibridged $\text{Co}_2(\text{CO})_7$ has not been described in the literature. More theoretical work is underway related to the structures and interconversions of this species.

The entire proposed pathway of the ketene formation and elimination steps are summarized in Fig. 7.

On the $\text{Co}_2(\text{CO})_7(\text{O}=\text{C}=\text{CHCO}_2\text{Et})$ potential energy hypersurface yet another ketene adduct **11** has been found with an unusual coordination mode. In this complex, which is only by 0.7 kcal/mol higher in free energy than **9**, the ketene ligand is mainly bound by the carbonyl oxygen revealing a Co–O bond distance of 2.039 \AA . On the other hand the coordination of the ketene carbon is also noticeable. Although the Co–C bond distance is relatively large, the C–C–O bond angle is 146° , significantly deviating from 180° , indicating a weak coordination of carbon towards Co2.

In order to shed some light on the coordination of ethoxycarbonylketene ligand in the more stable saturated complexes **7**, **9**, and **11**, the nature of interaction is studied within the framework of Charge Decomposition Analysis (CDA), developed by Dapprich and Frenking [15]. For all calculations $\text{O}=\text{C}=\text{CHCO}_2\text{Et}$ was considered as the donor fragment, whereas $\text{Co}_2(\text{CO})_7$ was considered as the acceptor fragment. The results are given in Table 7.

The small residual term for complexes **9**, and **11** indicate that the ligand is bound to the transition metal in a classical donor–acceptor manner. The slightly higher Δ value, however, for complex **7**, as well as the low amount of back-donation and the unusually high interaction energy suggest that **7** has some of covalent metallacycle character as well. On the other hand all the CDA descriptors of complex **9** are remarkably similar to those found for Pt–olefin complexes [16].

The donation and back-donation values of each canonical orbital of a given complex may also provide valuable qualitative information about the donor–acceptor character. Interestingly, in case of complex **7** HOMO is mostly responsible for both donation and the slight back donation (see Fig. 8a). The electron donation in the $(\mu^1-\eta^2)$ complex **9** is mainly described by the HOMO–1 orbital (Fig. 8b) whereas the back-donation is described by HOMO–2 and the results suggest that both cobalt atoms are involved in it (Fig. 8c). The unusually high donation in complex **11** may be rationalized by the overlap of a filled orbital of the ethoxycarbonylketene moiety with mainly the unfilled d_{22} orbital of Co2 (Fig. 8d). For the back-donation the HOMO–1 orbital is mostly responsible which just like the HOMO–2 of **9** has a contribution on both cobalt atoms (Fig. 8e).

3. Discussion

In the catalytic carbonylation experiments under atmospheric pressure of carbon monoxide using $\text{Co}_2(\text{CO})_8$ as the catalyst precursor the prevailing complex in the reaction mixture is complex **2** if the applied $[\text{EDA}]/[\text{CO}]$ ratio in the experiment was >10 (see for example entry 4 in Table 1 and the joining text in the results section). It seems to be obvious that under these reaction conditions the formation of the diethyl malonate product occurs mainly according to the catalytic cycle: **B**. In order to check this assumption we compared the observed rates of DEM formation with those calculated for the various steps using the experimentally determined rate constants compiled in Scheme 5. From the experiments performed under atmospheric CO pressure we chose entry 2 of Table 1, where we have measured both the rate of DEM formation $[r_{\text{DEM}}(\text{obs})]$ and the composition of the cobalt complexes in the reaction mixture after 1, 2, and 3 h reaction time. The results of the comparison can be seen in Table 8. First we calculated the rate of complex **1** formation from the precursor $\text{Co}_2(\text{CO})_8$ and ethyl diazoacetate (EDA) as $r_1(\text{calcd}) = 0.0716 \times 10^{-5}\text{ mol/dm}^3\text{ s}$ (entry

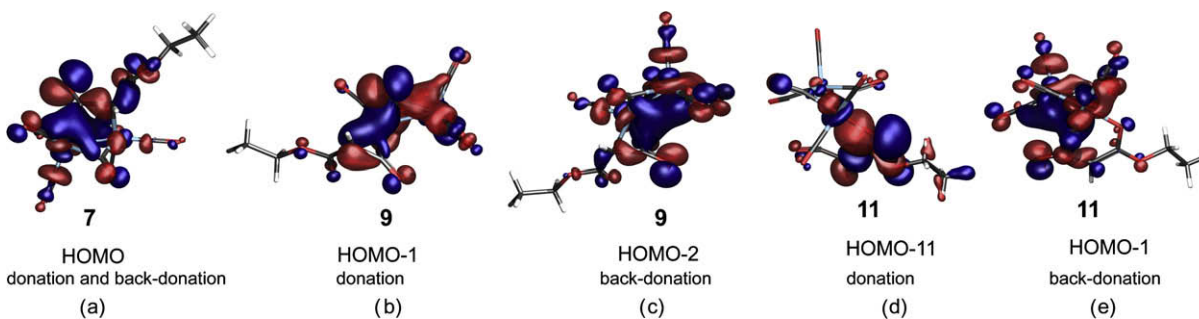


Fig. 8. Canonical molecular orbitals attributed to electron donation and back-donation in the coordinative saturated ketene complexes.

Table 8

The observed concentrations of diethyl malonate (DEM), $\text{Co}_2(\text{CO})_8$, $\text{Co}_2(\text{CO})_7(\text{CHCO}_2\text{Et})$ (**1**), and $\text{Co}_2(\text{CO})_6(\text{CHCO}_2\text{Et})_2$ (**2**), the observed rate of DEM formation ($r_{\text{DEM}} = [\text{DEM}]_t / t \times 3600$), the calculated rates of DEM formation $r_{\text{DEM}}^1 = k_{\text{DEM}}^1 / ([\mathbf{1}]_t [\text{CO}]_0)$ and $r_{\text{DEM}}^2 = k_{\text{DEM}}^2 / ([\mathbf{2}]_t [\text{CO}]_0)$, the calculated rates of complex **1** formation $r^1 = [\text{Co}_2(\text{CO})_8]_t / \{(k_{-1} [\text{CO}]_0 / k_1 k_2 [\text{EDA}]_t) + 1/k_1\}$ and the calculated rates of complex **2** formation $r^2 = [\mathbf{1}]_t / \{(k_{-1} [\text{CO}]_0 / k_1 k_2 [\text{EDA}]_t) + 1/k_1\}$ in the catalytic carbonylation reaction of ethyl diazoacetate $[\text{EDA}]_0 = 0.02 \text{ mol/dm}^3$ at 10°C under atmospheric pressure of CO, $[\text{CO}]_0 = 0.00509 \text{ mol/dm}^3$, applying $[\text{Co}_2(\text{CO})_8]_0 = 0.005 \text{ mol/dm}^3$ as the catalyst precursor in the presence of $[\text{Ethanol}]_0 = 0.05 \text{ mol/dm}^3$ using different reaction times (t). The experimentally determined rate constants k_{DEM}^1 , k_{DEM}^2 , $k_{-1}/k_1 k_2$, k_1 , $k_{-1}/k_1 k_2$, and k_1^1 were taken from Scheme 5.

Entry	Reaction time t (h)	$[\text{EDA}]_t / [\text{CO}]_0$	$[\text{DEM}]_t$ (mol/dm ³)	$[\text{Co}_2(\text{CO})_8]_t$ (mol/dm ³)	$[\mathbf{1}]_t$ (mol/dm ³)	$[\mathbf{2}]_t$ (mol/dm ³)	$10^5 \times r_{\text{DEM}}$ (obs) (mol/dm ³ s)	$10^5 \times r_{\text{DEM}}^1$ (calcd) (mol/dm ³ s)	$10^5 \times r_{\text{DEM}}^2$ (calcd) (mol/dm ³ s)	$10^5 \times r_1$ (calcd) (mol/dm ³ s)	$10^5 \times r_2$ (calcd) (mol/dm ³ s)
1	0	3.93	0	0.005	0	0				0.0716	
2	1	2.55	0.00094	0.0003	0.0033	0.0014	0.0261	0.0007	0.0188		0.0306
3	2	2.28	0.00178	0	0.0034	0.0016	0.0247	0.0007	0.0215		0.0282
4	3	2.11	0.00256	0	0.0033	0.0017	0.0237	0.0007	0.0228		0.0253

Table 9

The observed and calculated concentrations of diethyl malonate (DEM), $\text{Co}_2(\text{CO})_7(\text{CHCO}_2\text{Et})$ (**1**), and $\text{Co}_2(\text{CO})_6(\text{CHCO}_2\text{Et})_2$ (**2**) in the carbonyl cobalt-catalyzed carbonylation reaction of ethyl diazoacetate (EDA) in CH_2Cl_2 solution in the presence of ethanol at 10°C and 3 h reaction time using different initial concentrations. For the calculations the experimentally determined rate constants k_{DEM}^1 , k_{DEM}^2 , $k_{-1}/k_1 k_2$, k_1 , $k_{-1}/k_1 k_2$, and k_1^1 were taken from Scheme 5.

Entry ^a	$[\text{EDA}]_0$ (mol/dm ³)	$[\text{CO}]_0$ (mol/dm ³)	$[\text{EDA}]_0 / [\text{CO}]_0$	$[\text{Co}_2(\text{CO})_8]_0$ (mol/dm ³)	$[\text{DEM}]_{3\text{h}}$ (mol/dm ³)	$[\mathbf{1}]_{3\text{h}}$ obs ^b (mol/dm ³)	$[\mathbf{2}]_{3\text{h}}$ obs ^c (mol/dm ³)	$[\text{DEM}]_{3\text{h}}^{\text{d}}$ (mol/dm ³)	$[\text{DEM}]_{3\text{h}}^{\text{e}}$ (mol/dm ³)	$[\mathbf{1}]_{3\text{h}}$ calcd (mol/dm ³)	$[\mathbf{2}]_{3\text{h}}$ calcd (mol/dm ³)
25	0.500	0.3722	1.343	0.025	0.207	0.0140	0.0040	0.0137	0.2386	0.0121	0.0037
26	0.250	0.3722	0.672	0.025	0.087			0.0074	0.0649		
32	0.500	1.1211	0.446	0.025	0.111			0.0153	0.0883		
33	0.050	1.1211	0.0446	0.005	0.0067			0.000321	0.000186		
34	0.010	1.1211	0.0089	0.005	0.0019			0.0000644	0.0000075		

^a The numbers refer to entries in Table 1.

^b Determined by quantitative infrared spectroscopy at 1853 cm^{-1} .

^c Determined by quantitative infrared spectroscopy at 2080 cm^{-1} .

^d Calculated as $[\text{DEM}]_{3\text{h}}^{\text{d}} = (r_{\text{DEM}}^1)_{1.5\text{h}} \times 3 \times 3600$.

^e Calculated as $[\text{DEM}]_{3\text{h}}^{\text{e}} = (r_{\text{DEM}}^2)_{1.5\text{h}} \times 3 \times 3600$.

1 in Table 8), which is 2.88-times faster than the average rate of DEM formation. Therefore this step could not be the bottle-neck of the catalytic reaction. Then we calculated the rate of complex **2** formation from the precursor complex **1** and ethyl diazoacetate as r_2 (calcd) = 0.0306×10^{-5} (entry 2 in Table 8), 0.0282×10^{-5} (entry 3 in Table 8), and $0.0253 \times 10^{-5} \text{ mol/dm}^3 \text{ s}$ (entry 4 in Table 8) at 1, 2, and 3 h reaction time, respectively. Here again these rates are higher than the observed rate of DEM formation, hence the complex **2** formation is not rate determining either. The calculated rates of DEM formation $[r_{\text{DEM}}^1$ (calcd)] are much lower than the observed rates of DEM formation, but $[r_{\text{DEM}}^2$ (calcd)] are close to those. This means that these reactions are the bottle-necks of the catalytic reaction. Their ratio in the product formation is in the average 1:30. This means that the bulk of DEM is formed in the catalytic cycle **B**. The catalytic cycle **A** plays a minor role under the chosen experimental conditions. Especially the calculations from the concentrations in the third hour reaction time (entry 4 in Table 8) show that the sum of r_{DEM}^1 (calcd) = $0.0007 \times 10^{-5} \text{ mol/dm}^3 \text{ s}$ and r_{DEM}^2 (calcd) = $0.0228 \times 10^{-5} \text{ mol/dm}^3 \text{ s}$ is practically the same as the observed rate of DEM formation r_{DEM} (obs) = $0.0237 \times 10^{-5} \text{ mol/dm}^3 \text{ s}$. This result is in accord with the observation that in the low pressure range ($[\text{CO}] = 0.005\text{--}0.030 \text{ mol/dm}^3$) the catalytic reaction is first order with respect of carbon monoxide.

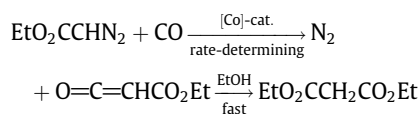
In order to explore the correlations in the high pressure range ($[\text{CO}] = 0.030\text{--}1.121 \text{ mol/dm}^3$) we performed calculations using the experimental initial concentrations of entries 25, 26, 32, 33, and 34 of Table 1. From the initial concentrations of $\text{Co}_2(\text{CO})_8$, EDA, and CO in these experiment we calculated the rate and the concentration of complex **1** formation using Eq. (13) as $r = [\text{Co}_2(\text{CO})_8]_0 / \{(k_{-1} [\text{CO}]_0 / k_1 k_2 [\text{EDA}]_0) + 1/k_1\}$ at the beginning and at half-time (1.5 h) of the reaction. From the half-time concentration of complex **1** we calculated the rate of diethyl malonate (DEM) formation in cycle **A** and its concentration ($[\text{DEM}]_{3\text{h}}^{\text{d}}$) and the rate of formation of

complex **2**. For the latter we used Eq. (17) as $r^1 = [\mathbf{1}]_t / \{(k_{-1} [\text{CO}]_0 / k_1 k_2 [\text{EDA}]_t) + 1/k_1\}$. From the half-time concentration of complex **2** we calculated the rate of DEM formation in cycle **B** and its concentration ($[\text{DEM}]_{3\text{h}}^{\text{e}}$). The results of the calculations are compiled in Table 9.

The data in Table 9 show that the diethyl malonate (DEM) formed in the experiments originates mainly in cycle **B** if the ratio of $[\text{EDA}]_0 / [\text{CO}]_0$ is higher than 0.1. On the other hand mainly cycle **A** is the source of DEM if the $[\text{EDA}]_0 / [\text{CO}]_0$ is below 0.1. In the former case the carbon monoxide concentration has a positive effect on the rate of DEM formation because the reactions of the complexes **1** and (mainly) **2** are the rate determining. In the latter case the carbon monoxide concentration has a negative effect on the rate of DEM formation because the formations of the complexes (mainly) **1** and **2** are the rate determining.

4. Conclusion

The presented results have proved that the catalytic carbonylation of ethyl diazoacetate in CH_2Cl_2 solution at 10°C in the presence of ethanol using $\text{Co}_2(\text{CO})_8$ as the catalyst precursor proceeds parallel in two different cycles **A** and **B** (see Scheme 5). Both catalytic cycles produce the intermediary ethoxycarbonylketene, which is scavenged in a fast reaction by ethanol to form diethyl malonate as the final organic product.



In the first cycle $\text{Co}_2(\text{CO})_7$ and $\text{Co}_2(\text{CO})_7(\text{CHCO}_2\text{Et})$ (**1**), whereas in the second one $\text{Co}_2(\text{CO})_6(\text{CHCO}_2\text{Et})$ and $\text{Co}_2(\text{CO})_6(\text{CHCO}_2\text{Et})_2$ (**2**) are the working repeating species. Source of $\text{Co}_2(\text{CO})_7$ in the first cycle is the catalyst precursor $\text{Co}_2(\text{CO})_8$. Complex $\text{Co}_2(\text{CO})_7(\text{CHCO}_2\text{Et})$

(1) is the source for $\text{Co}_2(\text{CO})_6(\text{CHCO}_2\text{Et})$ in the second cycle. The formation of the latter connects cycle A with cycle B. From the composition of the catalytic reaction mixtures and the observed kinetics of the individual steps in the cycles we conclude that using sufficient high concentration ratio of $[\text{N}_2\text{CHCO}_2\text{Et}]/[\text{CO}] \gg 0.1$, the rate-determining steps at low (1 bar) or high (50 bar) pressure of carbon monoxide are the reactions of $\text{Co}_2(\text{CO})_7(\text{CHCO}_2\text{Et})$ (1) and $\text{Co}_2(\text{CO})_6(\text{CHCO}_2\text{Et})_2$ (2) with carbon monoxide. Complex 2 is 66-times more effective than complex 1 in this reaction. At low concentration ratio $[\text{N}_2\text{CHCO}_2\text{Et}]/[\text{CO}] < 0.1$, the reactions of the catalyst precursors $\text{Co}_2(\text{CO})_8$ and complex 1 with ethyl diazoacetate become rate determining, in which reactions the carbon monoxide concentration has a negative effect. If the low concentration ratio of $[\text{N}_2\text{CHCO}_2\text{Et}]/[\text{CO}]$ is combined with a high CO concentration (for example at 150 bar pressure), more diethyl malonate is produced in catalytic cycle A than in catalytic cycle B.

Computational studies on the ketene formation step have shown that the coupling of the bridging carbene ligand with a terminal CO ligand takes place via a low barrier resulting in a coordinative unsaturated ketene complex, which is converted to a $(\mu^2-\eta^2)$ ketene complex by an uptake of external CO. The $(\mu^2-\eta^2)$ complex quickly transforms to a $(\mu^1-\eta^2)$ species which releases ethoxycarbonylketene via a small barrier resulting in the dibridged heptacarbonyl-dicobalt which reforms complex 1 after reacting with ethyl diazoacetate.

5. Experimental

5.1. General comments

Handling of the carbonyl cobalt complexes was carried out in an atmosphere of dry (P_4O_{10}) and deoxygenated (BTS contact, room temp.) argon or carbon monoxide utilizing standard Schlenk techniques [17]. Methylene chloride were dried and distilled under an atmosphere of argon or carbon monoxide according to standard procedures [18]. IR spectra were recorded on Thermo Nicolet Avatar 330 and Bruker Tensor 27 FTIR spectrometers using 0.00265, 0.00765, 0.0218 or 0.05097 cm CaF_2 solution cells, calibrated by the interference method [19]. Octacarbonyl dicobalt [20] and the μ_2 -ethoxycarbonylcarbene complexes 1 [2] and 2 [2] were prepared by literature procedures. Carbon monoxide was obtained from Messer Hungary.

5.2. Measurements at atmospheric pressure

The reactions of $\text{Co}_2(\text{CO})_8$, complex 1 and complex 2 with ethyl diazoacetate and ethanol at atmospheric pressure was performed in a thermostatted glass reactor connected to a gas burette under an atmosphere of carbon monoxide or argon. The gas volume change was followed by reading the gas burette in appropriate time intervals (usually 8–15 readings for calculation of the initial rates). The concentration of diethyl malonate, $\text{Co}_2(\text{CO})_8$, complex 1 and complex 2 in samples of the reaction mixture was calculated from the IR spectrum using the molar absorbances of diethyl malonate $\epsilon_M(\text{CH}_2\text{Cl}_2, 1749 \text{ cm}^{-1}) = 579 \text{ cm}^2/\text{mmol}$ and $\epsilon_M(\text{CH}_2\text{Cl}_2, 1732 \text{ cm}^{-1}) = 666 \text{ cm}^2/\text{mmol}$, $\text{Co}_2(\text{CO})_8$ $\epsilon_M(\text{CH}_2\text{Cl}_2, 2022 \text{ cm}^{-1}) = 697 \text{ cm}^2/\text{mmol}$, complex 1 $\epsilon_M(\text{CH}_2\text{Cl}_2, 1853 \text{ cm}^{-1}) = 953 \text{ cm}^2/\text{mmol}$, complex 2 $\epsilon_M(\text{CH}_2\text{Cl}_2, 2080 \text{ cm}^{-1}) = 3768 \text{ cm}^2/\text{mmol}$.

5.3. Measurements at higher than atmospheric pressure

Reactions above the atmospheric pressure using CO pressures were performed in a thermostatted stainless steel autoclave of 20 cm^3 capacity. The concentration of the components in the reaction mixture was determined from samples by quantitative infrared spectroscopy (see above).

5.4. Computational details

Full geometry optimizations have been performed at the density functional level of theory without any symmetry constraints using the GAUSSIAN 03 suite of programs [21]. For all the calculations the gradient-corrected exchange functional developed by Becke [22] was utilized in combination with a correlation functional developed by Perdew [23] and denoted as BP86. For cobalt the valence triple- ζ SDD basis set following the $(8s7p6d1f) \rightarrow [6s5p3d1f]$ contraction pattern is utilized with the corresponding relativistic effective core potential [24]. For the other atoms the 6-31G(d,p) basis set [25] was used. The density fitting basis sets were generated automatically from the AO primitives by the GAUSSIAN 03 program. The stationary points were characterized by frequency calculations in order to verify that they have zero imaginary frequencies for equilibrium geometries and one imaginary frequency for transition states. Thermochemistry corrections were taken from frequency calculations at 298.15 K and 1 atm. Intrinsic reaction coordinate (IRC) analyses [26] were carried out throughout the reaction pathways to confirm that the stationary points are smoothly connected to each other. For charge decomposition analyses (CDA) the AOMIX software was used [27].

Acknowledgements

The authors thank the Hungarian Academy of Sciences and the Hungarian Scientific Research Fund for financial support under Grant Nos. OTKA NK 71906 and F046959 and also thank the Supercomputer Center of the National Information Infrastructure Development (NIIF) Program as well as Flextra Lab KFT. The support of Bolyai Grant of the Hungarian Academy of Sciences for T.K. is also acknowledged.

References

- [1] N. Ungvári, T. Kégl, F. Ungváry, J. Mol. Catal. A: Chem. 219 (2004) 7.
- [2] R. Tuba, F. Ungváry, J. Mol. Catal. A: Chem. 203 (2003) 59.
- [3] N. Ungvári, F. Ungváry, in: L. Kollár (Ed.), Modern Carbonylation Methods, Wiley-VCH, Weinheim, 2008, p. 199 (Chapter 8).
- [4] E. Fördös, R. Tuba, L. Párkányi, T. Kégl, F. Ungváry, Eur. J. Org. Chem. (2009) 1994.
- [5] R. Tuba, E. Fördös, F. Ungváry, J. Mol. Catal. A: Chem. 236 (2005) 113.
- [6] E. Fördös, N. Ungvári, L. Párkányi, G. Szalontai, T. Kégl, F. Ungváry, Inorg. Chim. Acta 361 (2008) 1832.
- [7] N. Ungvári, E. Fördös, T. Kégl, F. Ungváry, Inorg. Chim. Acta 362 (2009) 1333.
- [8] R. Tuba, E. Fördös, F. Ungváry, Inorg. Chim. Acta 358 (2005) 4081.
- [9] A. Jonasson, O. Persson, P. Rasmussen, J. Chem. Eng. Data 45 (2000) 642.
- [10] M.P. Magee, H.-Q. Li, O. Morgan, W.H. Hersh, Dalton Trans. (2003) 387.
- [11] E. Fördös, N. Ungvári, T. Kégl, F. Ungváry, Eur. J. Inorg. Chem. (2006) 1875.
- [12] J.P. Kenny, R.B. King, H.F. Schaefer III, Inorg. Chem. 40 (2001) 900.
- [13] T. Kégl, F. Ungváry, J. Organomet. Chem. 692 (2007) 1825.
- [14] X. Feng, C. Xie, Z. Liu, Y. Xie, R.B. King, H.F. Schaefer III, Dalton Trans. (2009) 2599.
- [15] S. Dapprich, G. Frenking, J. Phys. Chem. 99 (1995) 9352.
- [16] A. Bedekovits, L. Kollár, T. Kégl, Inorg. Chim. Acta (submitted for publication).
- [17] D.F. Shriver, The Manipulation of Air-Sensitive Compounds, Krieger, Malabar, FL, 1982.
- [18] W.L.F. Armarego, D.D. Perrin, Purification of Laboratory Chemicals, 4th ed., Butterworth-Heinemann, Oxford, 1996.
- [19] H.H. Willard, L.L. Merritt Jr., J.A. Dean, F.A. Settle Jr., Instrumental Methods of Analysis, 6th ed., Wadsworth, Belmont, CA, 1981.
- [20] P. Szabó, L. Markó, G. Bor, Chem. Techn. (Leipzig) 13 (1961) 549.
- [21] GAUSSIAN 03, Revision B.05, M.J. Frisch, G.W. Trucks, H.B. Schlegel, G.E. Scuseria, M.A. Robb, J.R. Cheeseman, J.A. Montgomery Jr., T. Vreven, K.N. Kudin, J.C. Burant, J.M. Millam, S.S. Iyengar, J. Tomasi, V. Barone, B. Mennucci, M. Cossi, G. Scalmani, N. Rega, G.A. Petersson, H. Nakatsuji, M. Hada, M. Ehara, K. Toyota, R. Fukuda, J. Hasegawa, M. Ishida, T. Nakajima, Y. Honda, O. Kitao, H. Nakai, M. Klene, X. Li, J.E. Knox, H.P. Hratchian, J.B. Cross, C. Adamo, J. Jaramillo, R. Gomperts, R.E. Stratmann, O. Yazyev, A.J. Austin, R. Cammi, C. Pomelli, J.W. Ochterski, P.Y. Ayala, K. Morokuma, G.A. Voth, P. Salvador, J.J. Dannenberg, V.G. Zakrzewski, S. Dapprich, A.D. Daniels, M.C. Strain, O. Farkas, D.K. Malick, A.D. Clifford, K. Raghavachari, J.B. Foresman, J.V. Ortiz, Q. Cui, A.G. Baboul, S. Clifford, J. Cioslowski, B.B. Stefanov, G. Liu, A. Liashenko, P. Piskorz, I. Komaromi, R.L. Martin, D.J. Fox, T. Keith, M.A. Al-Laham, C.Y. Peng, A.

- Nanayakkara, M. Challacombe, P.M.W. Gill, B. Johnson, W. Chen, M. W. Wong, C. Gonzalez, J.A. Pople, Gaussian Inc., Pittsburgh, PA, 2003.
- [22] A.D. Becke, Phys. Rev. A 38 (1988) 3098.
- [23] J.P. Perdew, Phys. Rev. B 33 (1986) 8822.
- [24] M. Dolg, H. Stoll, H. Preuss, R.M. Pitzer, J. Phys. Chem. 97(1993) 5852.
- [25] W.J. Hehre, R. Ditchfield, J.A. Pople, J. Chem. Phys. 56 (1972) 2257.
- [26] C. Gonzalez, H.B. Schlegel, J. Chem. Phys. 90 (1989) 2154.
- [27] (a) S.I. Gorelsky, AOMIX: Program for Molecular Orbital Analysis, <http://www.sg-chem.net/>, University of Ottawa, 2009;
- (b) S.I. Gorelsky, A.B.P. Lever, J. Organomet. Chem. 635 (2001) 187.